

Two novel 2-D Lanthanide-Cadmium hetreometal-organic frameworks based on nanosized heart-like $\text{Ln}_6\text{Cd}_6\text{O}_{12}$ wheel-cluster exhibiting the luminescence sensing to the polarization and concentration of cations

Qi Liu,^a Su-Zhi Ge,^a Jie-Ceng Zhong,^a Yan-Qiong Sun^{*a,b} and Yi-Ping Chen^a

^a Department of Chemistry, Fuzhou University, Fuzhou, Fujian 350108, People's Republic of China. Fax: +86-591- 22866340; E-mail sunyq@fzu.edu.cn

^b State Key Laboratory of Structural Chemistry, Fujian Institute of Research on the Structure of Matter, Chinese Academy of Sciences, Fuzhou, Fujian 350002, PR China

Electronic Supplementary Information:

X-ray Crystallography. Suitable single crystals were selected and mounted on a glass fiber. All data of **1** were collected on a Rigaku Saturn 724 CCD diffractometer with graphite-monochromated MoK α ($\lambda = 0.71073 \text{ \AA}$) radiation in the ω scanning mode at room temperature; All data of **2** were collected on a Mercury CCD/AFC diffractometer with graphite-monochromated CuK α ($\lambda = 1.5418 \text{ \AA}$) radiation in the ω scanning mode at room temperature. The structures were solved by direct methods and refined by full-matrix least squares on F^2 using the SHELXTL-97 program package. Hydrogen atoms bond N and C were generated geometrically (C-H = 0.93 \AA , N-H=0.86 \AA) and refined with fixed isotropic displacement parameters. Powder X-ray diffraction (PXRD) patterns were recorded on an X'pert Pro diffractometer (CuK α).

Materials and General Details. Commercially available solvents and chemicals were used without further purification. IR spectra were measured as KBr pellets on a Perkin-Elmer Spectrum 2000 FT-IR in the range 400-4000 cm^{-1} . Thermogravimetric data were collected on a Mettler Toledo TGA/SDTA 851^e analyzer in flowing nitrogen at a heating rate of 10 °C/min. Luminescence measurements were made with an Edinburgh Instrument FS920 TCSPC luminescence spectrometer on powder crystal material of the compounds. The EDTA emission was measured in aqueous solvent with 0.0001M. The **2** solvent emissions were prepared by introducing **2** powder (5 mg) into DMF, acetone, ethanol, acetonitrile, aqueous ammonia, ethylenediamine, 1,2-propane diamine, pyridine, diethlenetriamine(DETA), triethylenetetramine(TETA), tetraethylenepentamine(TEPA), triethylamine, ethanolamine and water(5.00 mL) at room temperature. Similarly, the powder of **2** was immersed in aqueous solution containing different concentrations of M(NO_3)_x (M = Ag⁺, Mg²⁺, La³⁺, Ce³⁺, Zn²⁺, Cd²⁺, Pb²⁺, Al³⁺, Sm³⁺, Gd³⁺, Cu²⁺, Co²⁺, Cr³⁺, Fe³⁺, Ni²⁺ and Er³⁺) and 0.1M of NaNO₃, Na₂SO₄ and Na₃PO₄. Samples were prepared by introducing **2** powder (5 mg) into aqueous solution(5.00 mL) at room temperature, too. Before luminescence measurements, the suspensions were oscillated for 10 min using ultrasonic waves to ensure uniform dispersion. *UV-vis* spectra were recorded on a Perkin-Elmer Lambda 900 in the aqueous solutions of different cations and nitrogenous compounds.

Syntheses of **1** and **2**: A mixture of Ln_2O_3 (Sm_2O_3 , 0.0492 g, 0.141 mmol; Eu_2O_3 , 0.0495 g, 0.141 mmol), H_4EDTA (0.0802 g, 0.274 mmol), $3\text{CdSO}_4 \cdot 8\text{H}_2\text{O}$ (0.0495 g, 0.064 mmol) and 10 mL H_2O was sealed in a 25 mL stainless steel reactor with teflon liner and heated at 170 °C for 7 days and then the resulting solution was filtered to evaporate. Colorless prismatic crystals of **1** and **2** were recovered a few days later, washed with distilled water and dried in air, respectively. Yield: 20% (**1**) and 20%(**2**) (based on Ln_2O_3). Anal. calc. for $\text{C}_{30}\text{N}_6\text{O}_{49}\text{H}_{86}\text{Cd}_3\text{Sm}_2$ **1**: C, 18.45; H, 4.44; N, 4.30. Found: C, 18.49; H, 4.37; N, 4.15%; for $\text{C}_{30}\text{N}_6\text{O}_{49}\text{H}_{86}\text{Cd}_3\text{Eu}_2$ **2**: C, 18.42; H, 4.43; N, 4.30. Found: C, 18.38; H, 4.40; N, 4.21%.

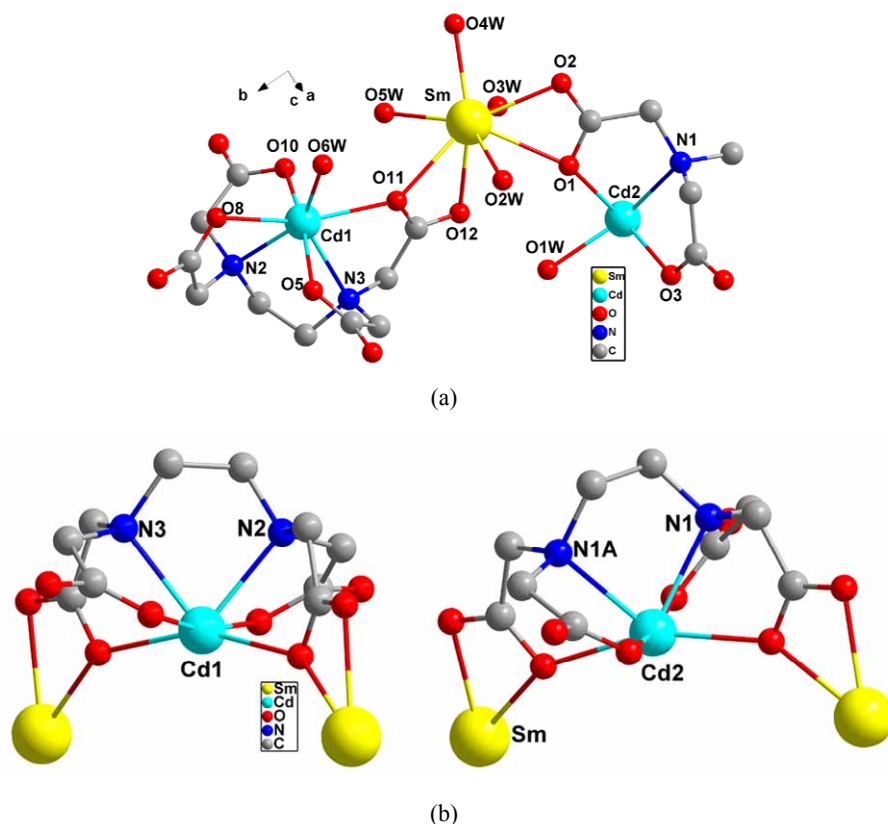


Fig. S1 (a) Ball-stick view of the asymmetrical unit of **1**. (b) The coordination modes of EDTA^{4-} in **1**.

As shown in Fig S1, in the asymmetrical unit of **1**, there is one unique Sm^{3+} , one and a half Cd^{2+} , five and a half coordinated water molecules and one and a half EDTA^{4-} anions, respectively. The two types of EDTA^{4-} adopt the same coordination modes, connecting two Sm^{3+} ions in two bidentate fashions and one Cd^{2+} ions in hexadentate chelating mode, which has rarely been observed in previous reports.

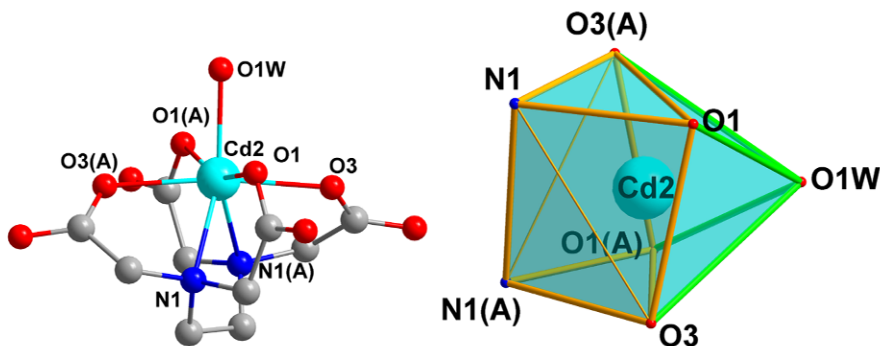


Fig. S2 The coordination environments of Cd atom in **1**. (left) The ball-stick representation; (right) The polyhedral representation. Atoms having “A” in their labels are symmetry-generated. A: 2-x, y, 2-z.

The coordination geometry for the two seven-coordinate Cd^{2+} ion is close to a monocapped trigonal prism: four O_{COO^-} and two N atoms from one EDTA^{4-} units as well as one terminal water molecule.

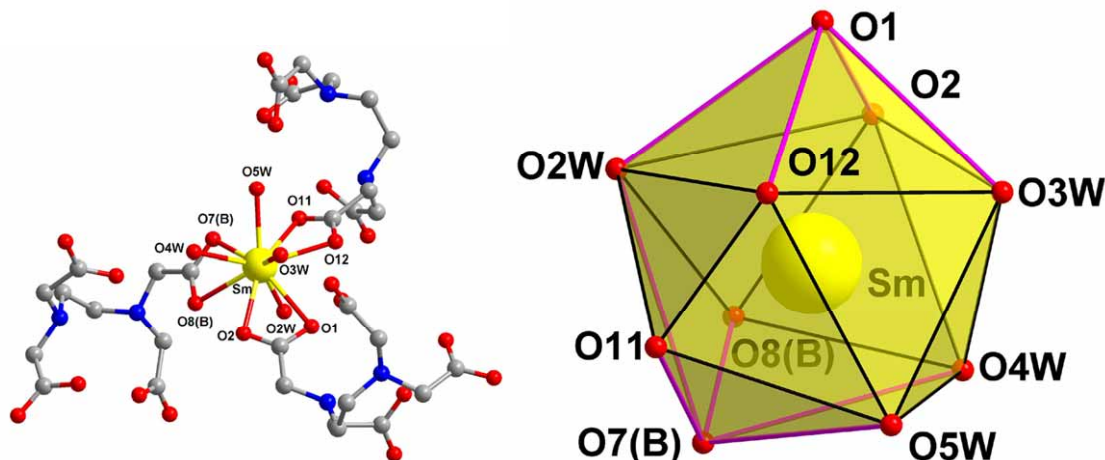


Fig. S3 The coordination environments of Sm atom in **1**. (left) The ball-stick representation. (right) The polyhedral representation. Atoms having “B” in their labels are symmetry-generated. B: $1.5-x, 0.5+y, 1-z$.

The Sm³⁺ ion is ten-coordinate and described as seriously distorted dicapped square antiprism: six O_{COO}⁻ from three EDTA⁴⁻ units and four terminal water molecules (Fig. S3).

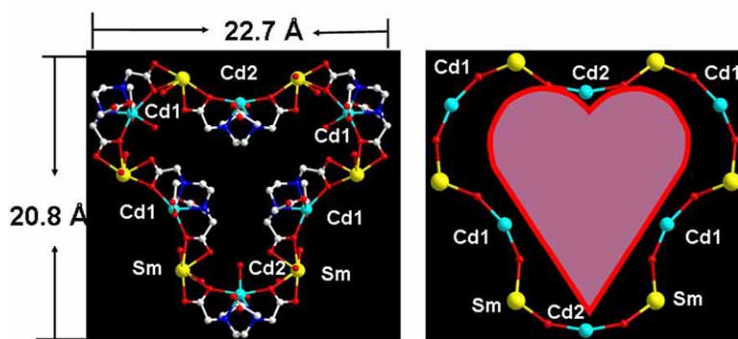


Fig. S4 (left) Ball-stick view of the nanosized heart-like Ln_6Cd_6 12-membered ring. (right) Ball-stick view of the nanosized heart-like $\text{Ln}_6\text{Cd}_6\text{O}_{12}$ wheel-cluster. Color code: Sm, yellow; Cd, cyan; O, red; C, white; N, blue.

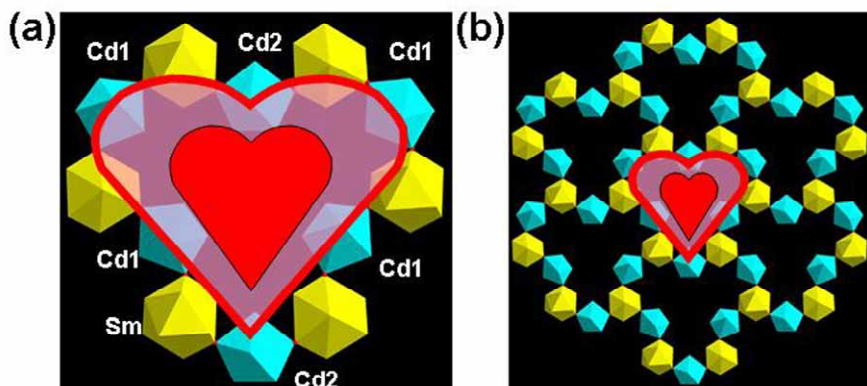


Fig. S5 (a) Polyhedral view of the nanosized heart-like $\text{Ln}_6\text{Cd}_6\text{O}_{12}$ wheel-cluster. (b) Polyhedral view of layered network of $\text{Ln}_6\text{Cd}_6\text{O}_{12}$ wheels. Color code: Sm, yellow; Cd, cyan; O, red.

Six SmO_{10} and six CdO_5N_2 polyhedrons are alternately connected through bridging the $\mu_2\text{-O}$ to form a Ln-Cd heterometallic $\text{Ln}_6\text{Cd}_6\text{O}_{12}$ heart-like wheel-cluster (Fig. 1a, S4, S5), which is observed for the first time in Ln-Cd chemistry. The dimension of the $\text{Ln}_6\text{Cd}_6\text{O}_{12}$ ring is about $22.7 \times 20.8 \text{ \AA}$ (Fig. S4). Each $\text{Ln}_6\text{Cd}_6\text{O}_{12}$ is linked to six surrounding wheels by sharing Sm^{3+} , forming a highly ordered layered wheel-cluster network, which presents the first example two-dimensional layer Ln-Cd HMOFs (Fig. 1c, S5).

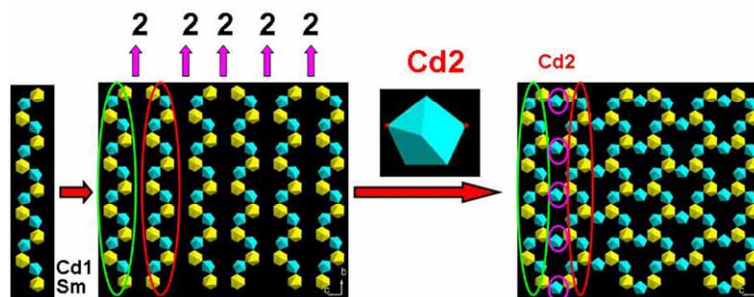


Fig. S6 2-D Ln-Cd wheel-cluster layer constructed from the inorganic heterometallic chiral helical chain made of $-\text{Sm}-\text{O}11-\text{Cd}1-\text{O}8-$ bridged by Cd2. Color code: Sm, yellow; Cd, cyan; O, red.

Remarkably, there are chiral helical cluster chains, which are only built up from Cd1 and Sm atoms alternately bridged by $\mu_2\text{-O}$ atoms (Fig. 1b). The shortest Cd···Sm distance is 4.83 \AA . The adjacent helical cluster chains related by two-fold axis are connected by Cd2 atoms which coordinated to $\mu_2\text{-O}$ atoms offered by SmO_{10} polyhedrons to generate 2D layer in the bc plane (Fig. 1c, S6).

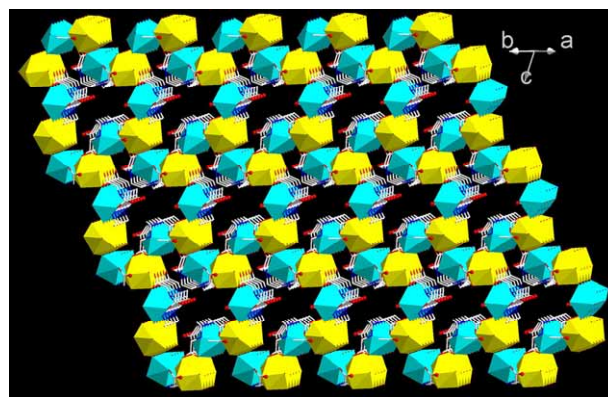


Fig. S7 The packing structure of 2D viewed along [110] direction. Color code: Sm, yellow; Cd, cyan; O, red; C, white; N, blue.

The 2D layers are further packed in $\cdots\text{AAA}\cdots$ stacking mode along the [110] direction and the free water molecules are suspended between the layers (Fig. 2, S7).

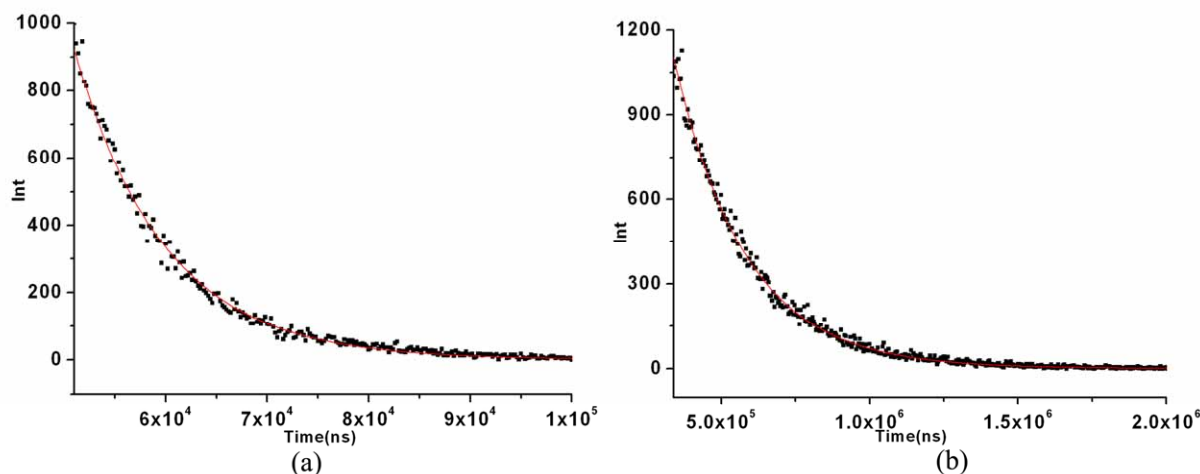


Fig. S8 The decay curve for **1** (a) ($\lambda_{\text{ex}} = 403 \text{ nm}$, $\lambda_{\text{em}} = 642 \text{ nm}$) and **2** (b) ($\lambda_{\text{ex}} = 394 \text{ nm}$, $\lambda_{\text{em}} = 618 \text{ nm}$) in the solid state at ambient temperature. The smooth red lines are the fitted curves.

The decay curves of fluorescence-emission for **1** (a) and **2** (b) were investigated. The luminescence decay curves were fitted with the single-exponential function: $F(t) = A + B_1 \exp(-t/T_1)$ for **1** and **2**. $T_1 = 8.855 \mu\text{s}$ for **1**, and $T_1 = 239.84 \mu\text{s}$ for **2**, respectively. The parameters were listed as following.

For compound **1**:

Fit Parameters

$$\text{Fit} = A + B_1 \exp(-t/T_1)$$

	Value	Std Dev		Value	Std Dev	Rel %
T_1	8.855E-6	4.806E-8	B_1	9.434E+2	6.821E+0	100.00
Chisq	1.468E+0		A	3.450E-1		

For compound **2**:

Fit Parameters

$$\text{Fit} = A + B_1 \exp(-t/T_1)$$

	Value	Std Dev		Value	Std Dev	Rel %
T_1	239.84E-6	1.01E-6	B_1	11.2309E+2	25.27E+0	100.00
Chisq	1.656E+0		A	4.920E-1		

The luminescence of **1** and **2** were measured in solid state at room temperature (Fig. 3). Complexes **1** and **2** present characteristic emission bands of Ln^{3+} ions and show broad emission in the 450–550 nm range which can be assigned to the luminescence of the Cd–ligand section (*d*-block). For the solid emission spectrum of **1**, the emissions at 562, 597 and 642 nm are attributed to the characteristic emission of ${}^4\text{G}_{5/2} \rightarrow {}^6\text{H}_J (J=5/2, 7/2 \text{ and } 9/2)$ of Sm^{3+} . The broad emission at 470–550 nm corresponds to the ligand(EDTA⁴⁻) to metal(Cd²⁺) charge transfer. For the solid emission spectrum of **2**, the emissions at 580, 593, 618, 650 and 696 nm are attributed to the characteristic emission of ${}^5\text{D}_0 \rightarrow {}^7\text{F}_J (J=0-4)$ of Eu^{3+} . The ${}^5\text{D}_0 \rightarrow {}^7\text{F}_0$ transition observed as a weak single peak at 580 nm

demonstrates the presence of only one site for the Eu³⁺ ion. The $^5D_0 \rightarrow ^7F_2$ transition is clearly stronger than the $^5D_0 \rightarrow ^7F_1$ transition, which indicates the absence of inversion symmetry at Eu³⁺ site. This is in agreement with the result of the single crystal X-ray analysis. It exhibits LMCT in **2**, too.

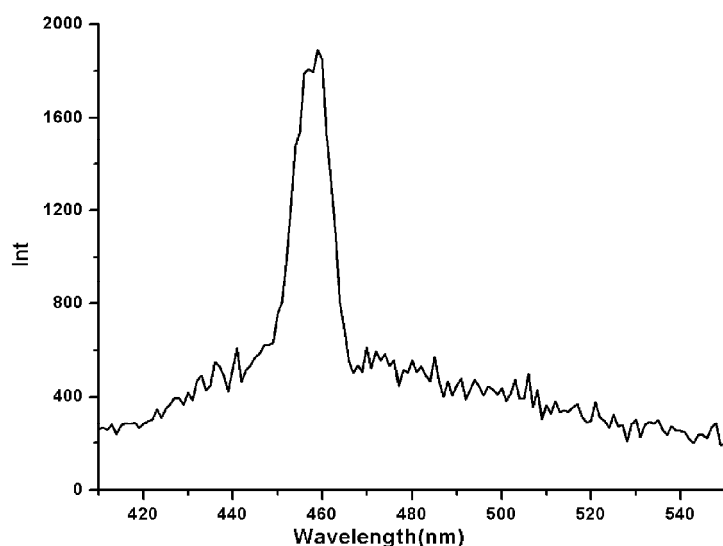


Fig. S9 Emission spectrum of H₄EDTA of 0.0001M aqueous solution(excitation at 395nm).

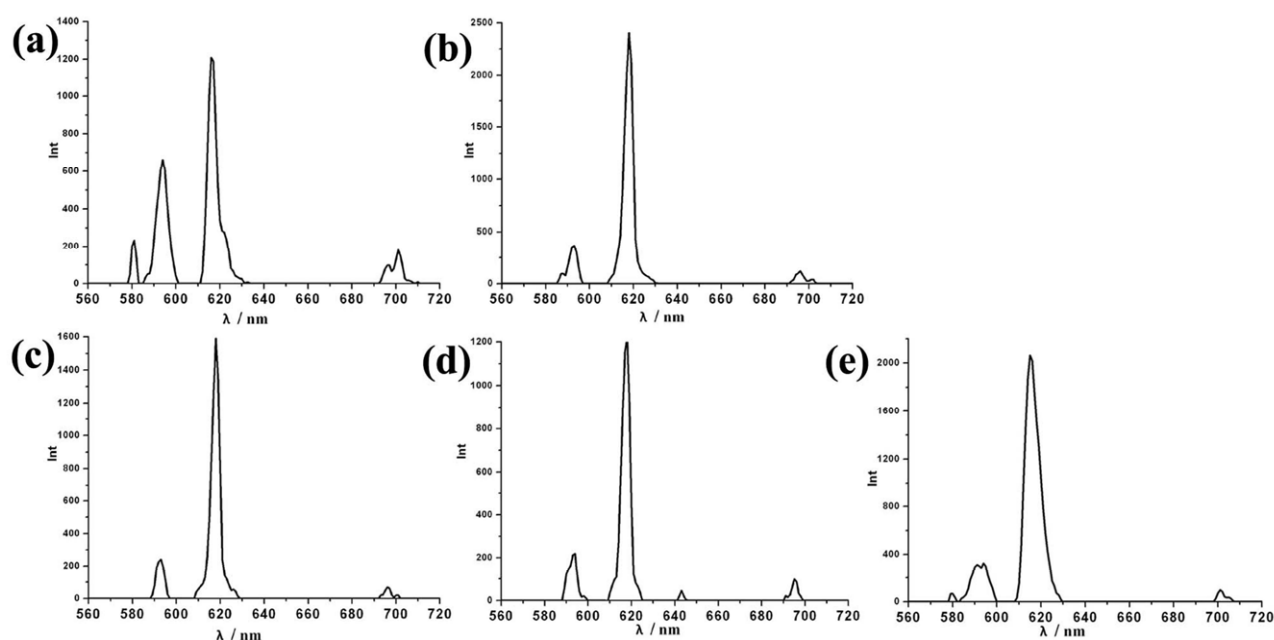


Fig. S10 The luminescence spectra of **2** in different solvents (excitation at 395 nm). (a)water, (b)ethanol, (c)acetonitrile, (d)acetone, (e)DMF.

The experiments of luminescent sensing of small molecules for **2** are performed. Because **2** is stable in common organic solvents and can be easily dispersed in them. Interestingly, compound **2** dispersed in water also shows characteristic emission bands of Eu(III) ions, but the intensity ratio (I) of $I(^5D_0 \rightarrow ^7F_2)$ (~594nm) : $I(^5D_0 \rightarrow ^7F_1)$ (~616nm) changed compared to that of in solid state ($I \approx 1.7$ in water and $I \approx 5$ in solid state, respectively). This could be contributed to the chelating of EDTA⁴⁻ anions to Eu³⁺ ions, which increases the stability of the complex and reduces the quenching effect of O-H vibration. For the solvents with the relatively high water content, such as ethanol, acetonitrile, acetone, and DMF, the luminescence spectra do not show too much difference from that

record in solid state, indicating that these solvents have no intense influence on the emission of **2**.

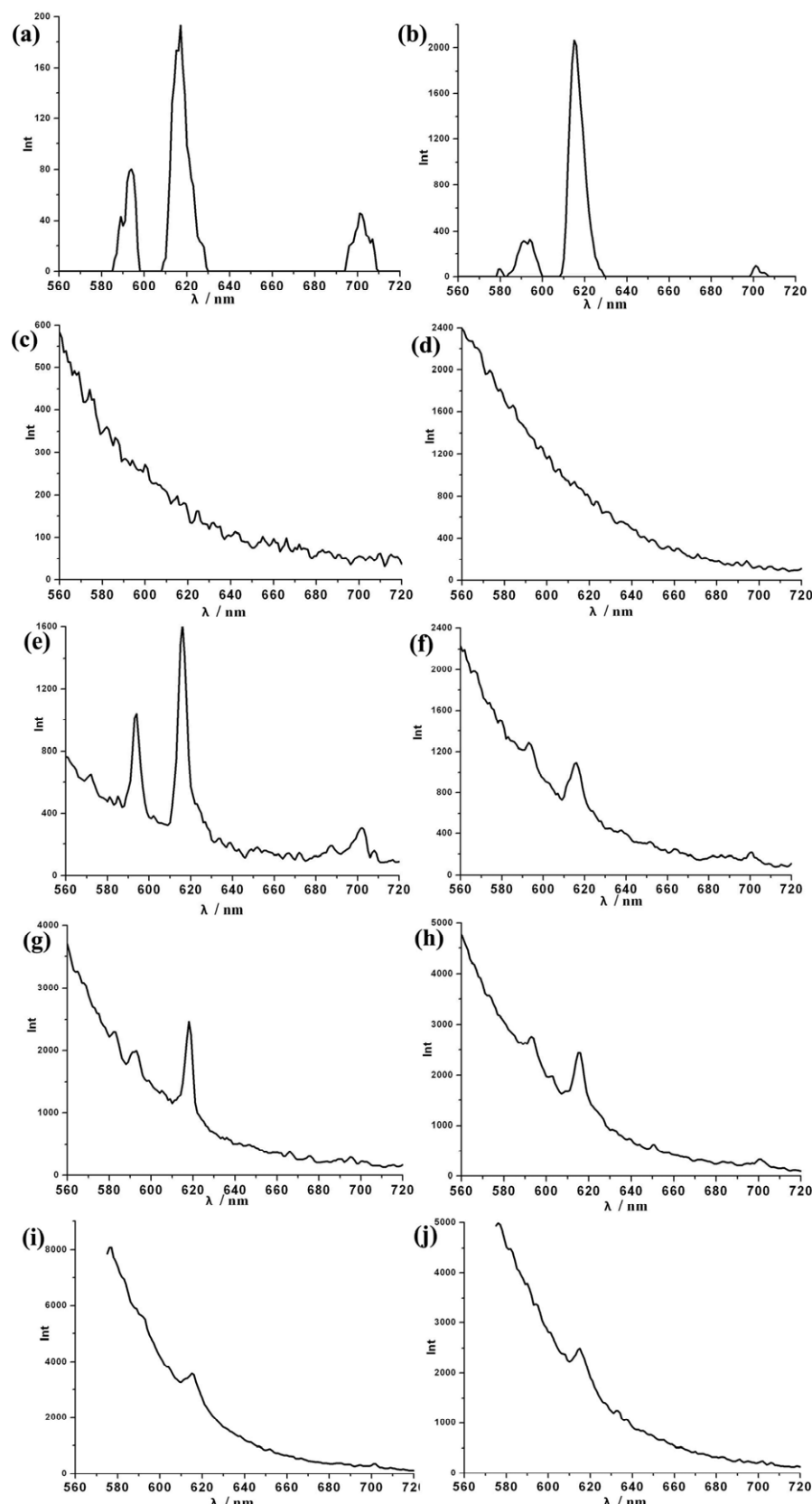


Fig. S11 The luminescence spectra of **2** in different nitrogenous compounds (excitation at 395 nm). (a) ammonia water, (b) DMF, (c) ethanolamine(EA), (d) triethylamine(TA), (e) ethylenediamine, (f) 1,2-propanediamine, (g) pyridine, (h) diethylenetriamine(DETA), (i)

triethylenetetramine(TETA), (j) tetraethylenepentamine(TEPA).

But for the solvents like ethylenediamine, 1,2-propane diamine, pyridine, diethylene triamine(DETA), triethylenetetramine(TETA), tetraethylenepentamine(TEPA), there are great reduce in the intensity of LS, especially the ethanolamine(EA) and triethylamine(TA) exhibit significant quenching of luminescence intensity which

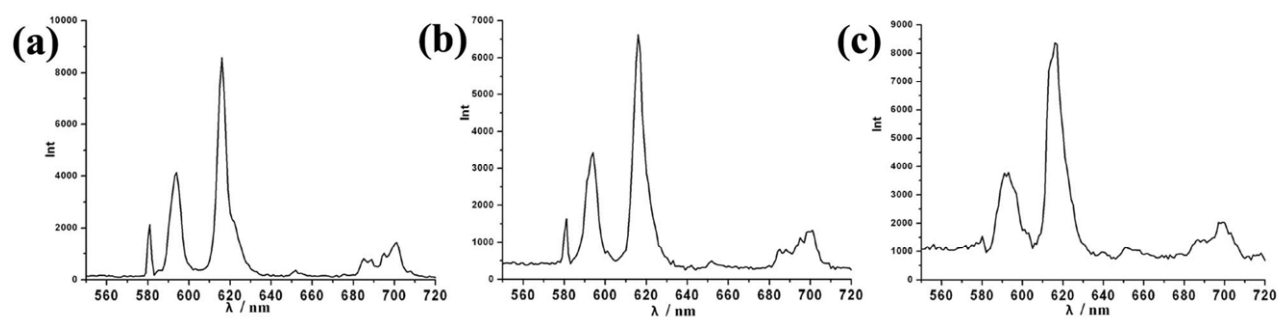
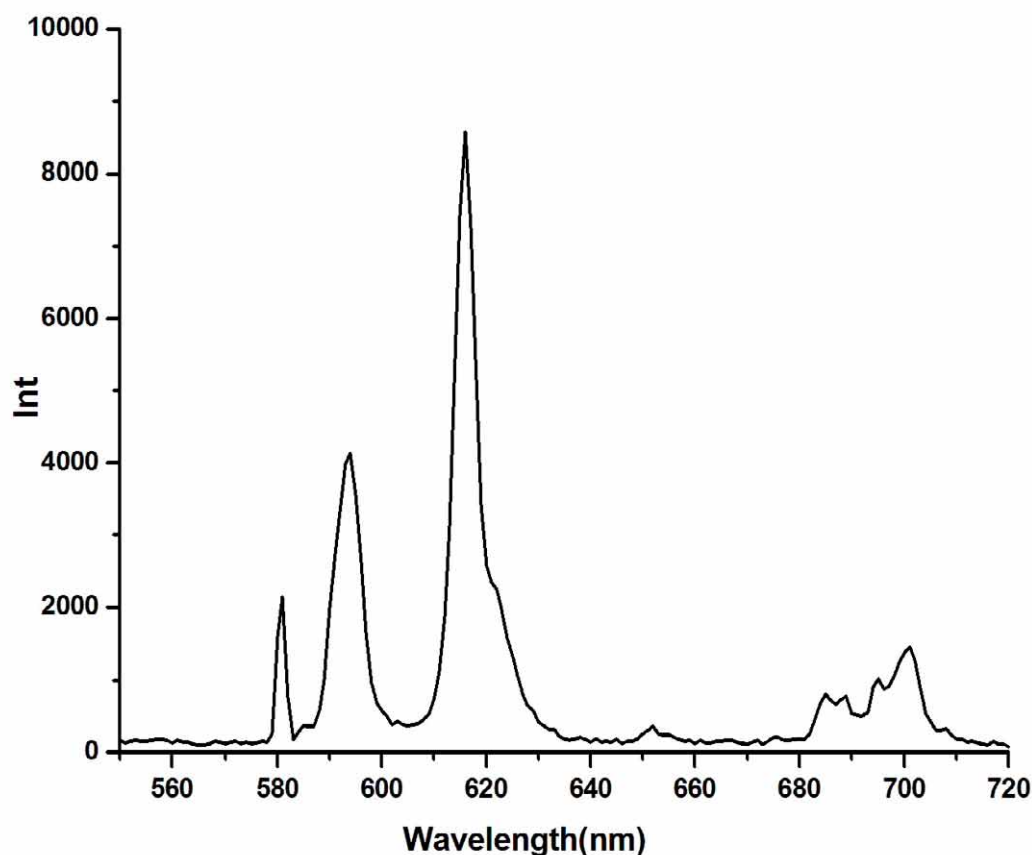


Fig. S13 The luminescence spectra of **2** in anions aqueous solution of 0.1M(excitation at 395 nm). (a) NaNO_3 , (b) Na_2SO_4 , (c) Na_3PO_4

The LS of powder samples of **2** dispersed in water solution containing different anions were recorded. The anions (NO_3^- , SO_4^{2-} , PO_4^{3-}) have no effect on the LS of **2**.

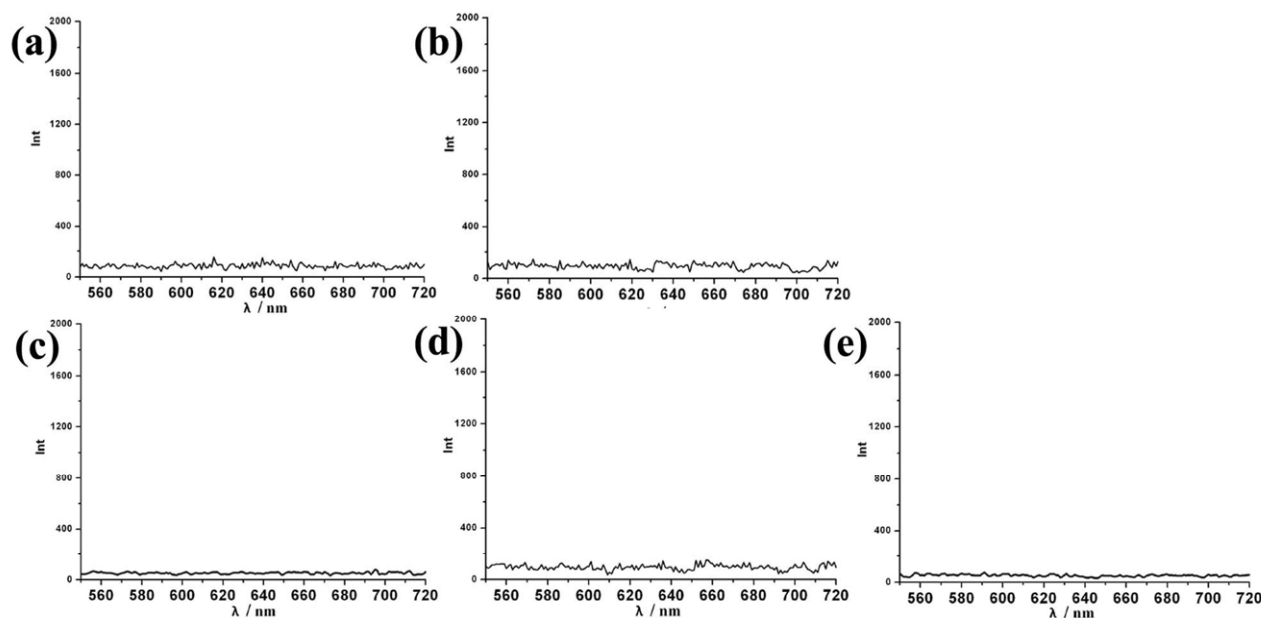


Fig. S14 The luminescence spectra of **2** in cations aqueous solution of 0.1M M(NO₃)_x(excitation at 395 nm). (a)Cr³⁺, (b)Fe³⁺, (c)Co²⁺, (d)Ni²⁺, (e)Cu²⁺

The LS completely quenched in water solution containing 0.1M of Cr³⁺, Fe³⁺, Co²⁺, Ni²⁺ and Cu²⁺ which have unpair electrons on *d*-orbitals whereas the LS of other cations including Ln³⁺ solutions don't, thus indicating the potential of **2** for the sensing of metal ions with unpair electrons on *d*-orbitals. The quenching effect of these metal ions may be attributed to the *d-d* transition for these metal ions with unpaired electrons by absorbing excitation lights or energy. For Ln³⁺ ions, though it exits unpaired ions on *f*-orbitals, the absorption coefficient is low for *f-f* transition which is symmetry forbidden.

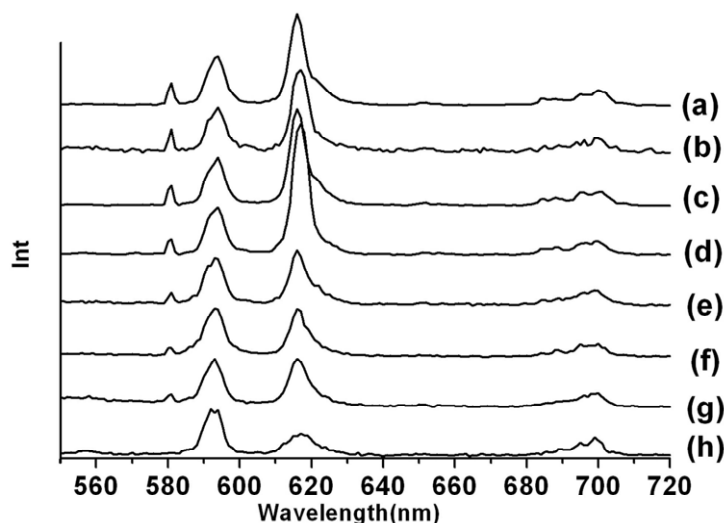


Fig. S15 The luminescence spectra of **2** in cations aqueous solution of 0.01M M(NO₃)_x(excitation at 395 nm). (a) La³⁺, (b) Ce³⁺, (c) Zn²⁺, (d) Cd²⁺, (e) Al³⁺, (f) Sm³⁺, (g) Gd³⁺, (h) Er³⁺.

Most interestingly, the intensity ratio (I) values of a $I(^5D_0 \rightarrow ^7F_2)(\sim 594\text{nm}) : I(^5D_0 \rightarrow ^7F_1)(\sim 616\text{nm})$ of the Eu³⁺ ion heavily dependent on the polarization of the cations and their concentration have been measured. The effect order should be La³⁺≈Ce³⁺≈Zn²⁺<Al³⁺<Sm³⁺≈Gd³⁺<Er³⁺ of 0.01M. This is almost in line with the

polarization of these cations.

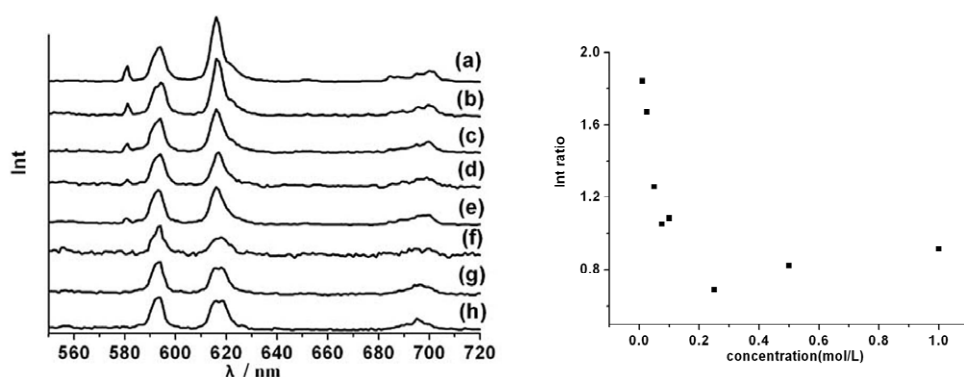


Fig. S16 (left) The luminescence spectra of **2** in Zn²⁺ aqueous solution of different concentration ($\lambda_{\text{ex}} = 395$ nm). (a)0.01M, (b) 0.025M, (c)0.05M, (d) 0.075M, (e) 0.1M, (f) 0.25M, (g)0.5M, (h)1M. (right) The relation between the intensity ratio (I) of $I(^5D_0 \rightarrow ^7F_2)$ (~594nm) : $I(^5D_0 \rightarrow ^7F_1)$ (~616nm) and the concentration of Zn²⁺ aqueous solution.

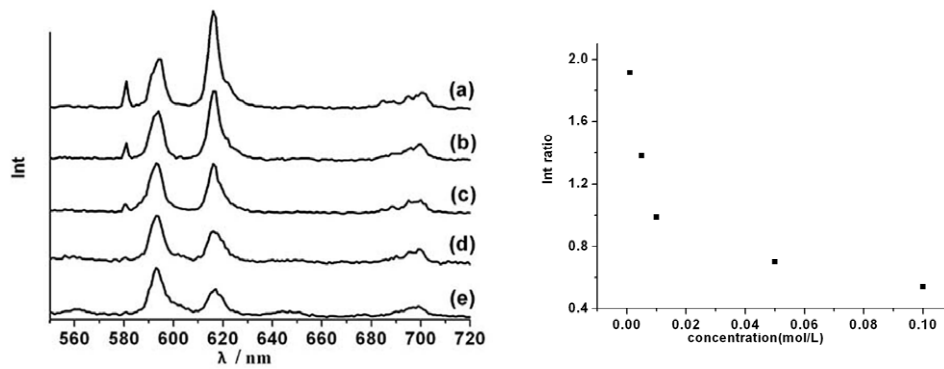


Fig. S17 (left) The luminescence spectra of **2** in Sm³⁺ aqueous solution of different concentration ($\lambda_{\text{ex}} = 395$ nm). (1)0.001M, (2)0.005M, (3)0.01M, (4)0.05M, (5)0.1M (right) The relation between the intensity ratio (I) of $I(^5D_0 \rightarrow ^7F_2)$ (~594nm) : $I(^5D_0 \rightarrow ^7F_1)$ (~616nm) and the concentration of Sm³⁺ aqueous solution.

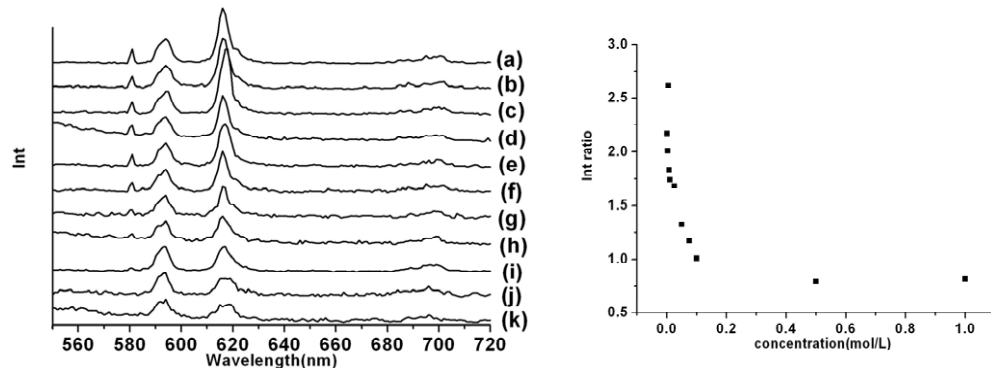


Fig. S18 (left) The luminescence spectra of **2** in Cd²⁺ aqueous solution of different concentration ($\lambda_{\text{ex}} = 395$ nm). (a)0.001M, (b) 0.0025M, (c)0.005M, (d) 0.0075M, (e) 0.01M, (f) 0.025M, (g)0.05M, (h)0.075M, (i) 0.1M, (j) 0.5M, (k) 1M. (right) The relation between the intensity ratio (I) of $I(^5D_0 \rightarrow ^7F_2)$ (~594nm) : $I(^5D_0 \rightarrow ^7F_1)$ (~616nm) and the concentration of Cd²⁺ aqueous solution.

The concentration of cations also affects this ratio. As shown, the intensity of $^5D_0 \rightarrow ^7F_2$ transition is larger than $^5D_0 \rightarrow ^7F_1$ transition in low concentration at first, then nearly equal, last smaller with the concentration increasing. The varied trends of I values of **2** with the concentration increasing in Zn²⁺, Sm³⁺, Cd²⁺ aqueous solutions are accordant.

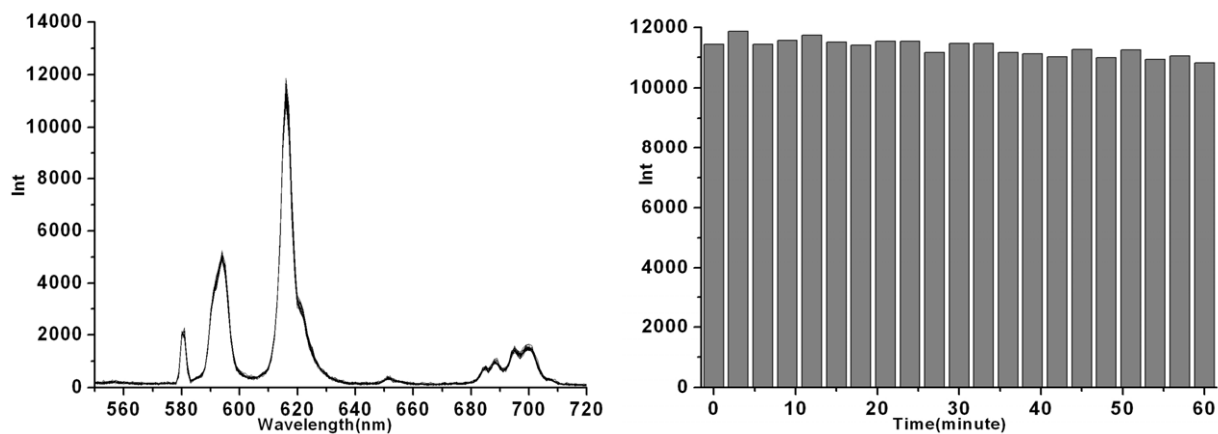


Fig. S19 (left) The emission spectra of **2** in Mg²⁺ aqueous solution measured every three minutes in an hour ($\lambda_{\text{ex}} = 395$ nm). (right) The emission intensity of ⁵D₀-⁷F₂ (616 nm) transition versus time.

The powder of compound **2** was introduced into Mg²⁺ aqueous solution, oscillated for 10 minutes using ultrasonic. Then luminescence spectra were collected every three minutes in an hour. As shown, the emission intensity nearly kept unchanged throughout the measurement. Plot a figure using the intensity of ⁵D₀-⁷F₂ (616 nm) versus time, (see right), the intensity remains unchanged in 60 minutes.

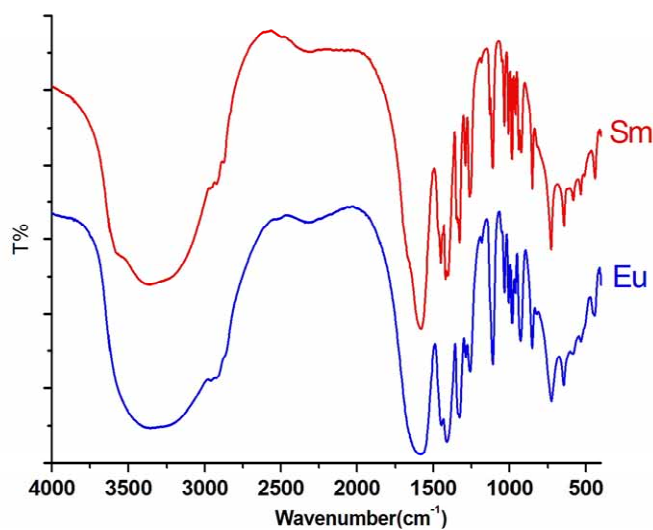


Fig. S20 IR spectra of **1**(Sm), **2**(Eu) respectively.

The two IR spectra are very similar with each other. The broad band at 3700-2650 cm⁻¹ corresponds to the stretching bands of O-H of water molecules. The band at 1585 cm⁻¹ corresponds to the stretching bands of C=O. The red shift of this band indicates the coordination between the metal ions and carboxylate radicals of EDTA⁴⁻.

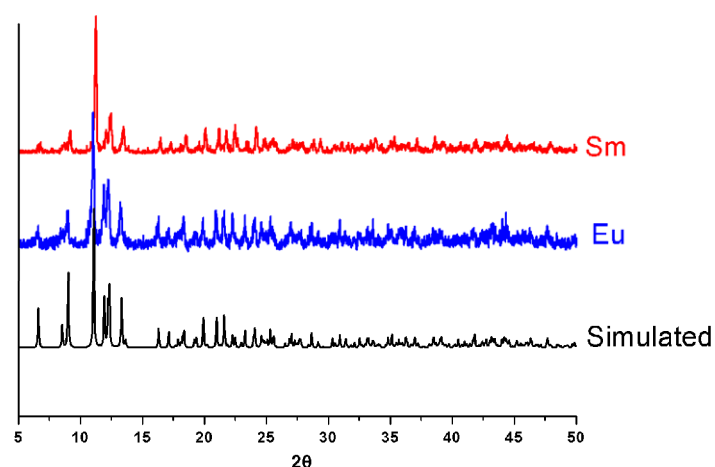


Fig. S21 The PXRD pattern of **1**(Sm), **2**(Eu) and simulated respectively.

The PXRD patterns of **1** and **2** are very close to each other, which coincide with simulated, indicating the purity of the crystals.

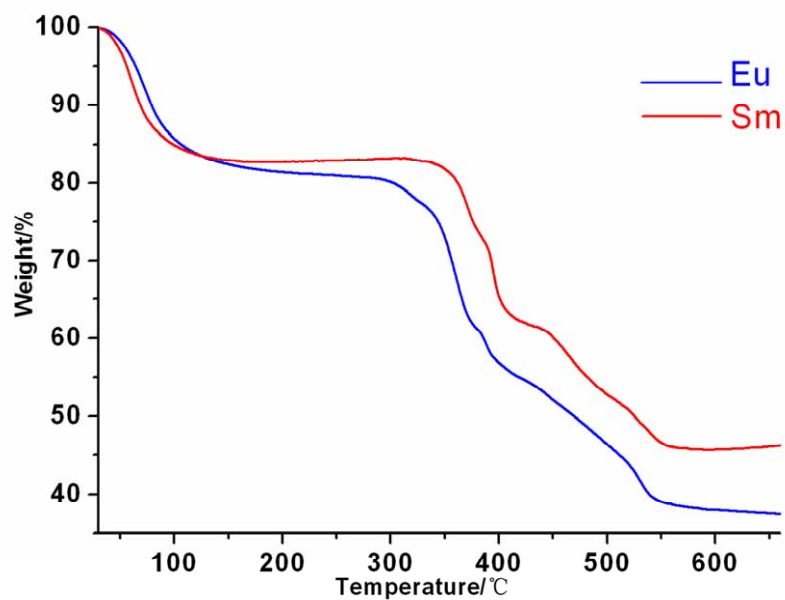


Fig. S22 TGA of **1** and **2**.

The thermal stability of **1** and **2** was examined by the TGA analysis in dry N₂ atmosphere from 30 to 700 °C. In the TGA curve, the weight loss of 17.14% (calcd: 17.51%) for **1**, 17.74% (calcd: 17.50%) for **2** in the temperature range 30–160 °C, corresponding to the successive release of 14 free water molecules and 5 coordinated water molecules per formula. The decomposition of H₄EDTA is observed from 160 °C to 660 °C. The residue might be Sm₂O₃·3CdO (calcd / found: 37.58% / 36.64%) for **1**, Eu₂O₃·3CdO (calcd / found: 37.68% / 37.41%) for **2**.

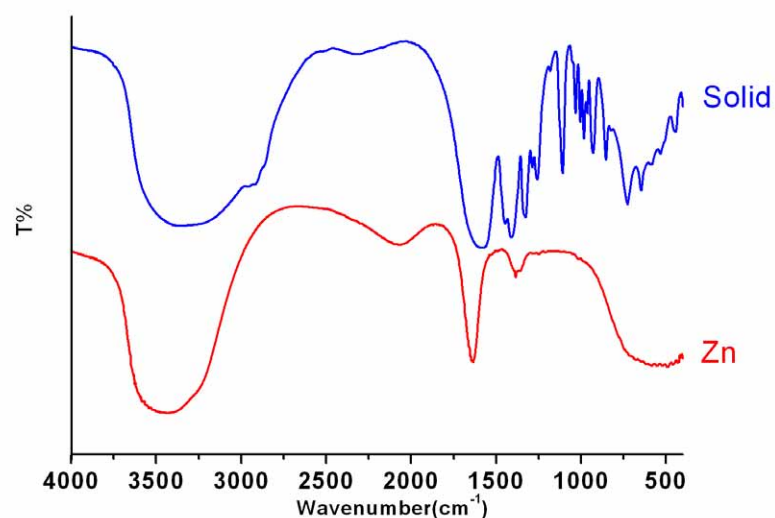


Fig. S23 IR spectra of **2** (blue) in solid state and **2** in the Zn^{2+} solution (red)